Environmental Processes (2026) 13:42
https://doi.org/10.1007/s40710-026-00851-0

RESEARCH

Model Based Groundwater Salinization Dynamics and Mechanisms in a Peaty Shallow Aquifer of the Po River Lowland (Italy)

Mattia Gaiolini[1] · Chiara Sbarbati[1] · Micòl Mastrocicco[2] · Nicolò Colombani[3]

Received: 13 May 2026 / Accepted: 30 June 2026

Abstract
The Po River (Italy) floodplain is a fragile environment extremely vulnerable to pollution and salinization risk. Here, freshwater availability for agricultural needs has become of concern and farmers are facing crops production decline due to droughts, increasing soil and groundwater salinity. To address salinization problems in complex systems, density dependent numerical flow and transport models are key tools. This study explored the role of stagnant zones, sorption and salt release from peats in modelling salinity dynamics in a coastal shallow aquifer. SEAWAT 4.2 was used to reproduce groundwater heads and salinity dynamics in two adjacent agricultural fields: a cultivated plot where groundwater and soil salinity are not yet reducing crop yields (model A1); and second field plot already unsuitable for cultivation (model A2). Both models were successful in grasping the magnitude and timing of groundwater level and salinity fluctuations over time. Transport models set-up with stagnant zones, sorption and salt release from peats best reproduced the observed trends in comparison to classical advection-dispersion equation simulations that overestimated salinity distribution within both plots. Sorption resulted to be crucial in representing the underlying processes of buffering and delaying salinity pulses, together with additional salt mass accounting for long-term source of salinity within peaty horizons. Mass budget calculations revealed high quantity of salt released from both the domains confirming the low efficiency of subirrigation in freshening these organic-rich peaty environments. This study improves the understanding of key phenomena driving salinization in these fragile lowlands, adding process realism and management relevance.

Keywords Transport modelling · Groundwater salinization · SEAWAT · Stagnant zones · Peats · Agricultural lowlands

✉ Nicolò Colombani
n.colombani@univpm.it

1 DEB - Department of Ecological and Biological Sciences, University of Tuscia, Largo Università snc, Viterbo 01100, Italy

2 DiSTABiF - Department of Environmental, Biological and Pharmaceutical Sciences and Technologies, Campania University “Luigi Vanvitelli”, Via Vivaldi 43, Caserta 81100, Italy

3 SIMAU - Department of Materials, Environmental Sciences and Urban Planning, Marche Polytechnic University, Via Brecce Bianche 12, Ancona 60131, Italy

Published online: 04 July 2026

1 Introduction

Salinization of water resources is becoming a major threat to agricultural sustainability in irrigated lowlands worldwide (Hussain et al. 2020; Khondoker et al. 2023; Sanga et al. 2024). In coastal and deltaic plains, groundwater and soil salinity are often associated with paleo seawater trapped into low-permeability lenses acting as long-term diffusion of salts and other contaminants (Dang et al. 2020; Seibert et al. 2023; Habakaramo Macumu et al. 2024). Moreover, in intensively cultivated and drained environments pre-existing brackish or saline conditions are often worsened by evapoconcentration of salts, relative sea-level rise and overexploitation of freshwater resources (Erostate et al. 2020).

In this context historical reclamation, together with hydrogeological and geomorphological changes within the Po River delta (Italy) made the entire floodplain extremely vulnerable to flooding and salinization risk (Colombani et al. 2017; Bonaldo et al. 2023). In addition, warmer and dryer summers during the crops growing seasons with reducing freshwater availability has become a concern for agricultural water managers (Gervasio et al. 2022) that are facing a decline in crop yields due to increasing soil and groundwater salinity (Zörb et al. 2019; Majeed and Muhammad 2019).

To address these problems, understanding and quantifying salinity dynamics is essential to protect agricultural productivity and guide long-term management of these fragile environments. Over the years numerical models have represented a key tool to clarify groundwater-related problems such as salinization in complex systems. Widely used numerical models like SEAWAT (Langevin 2009), SUTRA (Voss 1984) and FEFLOW (Diersch 2005) were successfully employed to simulate salinization processes in agricultural lowlands (Meyer et al. 2019; Yang et al. 2023; Gaiolini et al. 2025a). Despite their wide use, most applications of SEAWAT and related models simulate solute transport as a single domain process described by the classical advection-dispersion equation (ADE). This approach represents solute transport within a single mobile domain and does not explicitly account for mass transfer between mobile and immobile pore domain. As a result, ADE formulations may have difficulties reproducing transport behavior in highly heterogeneous media where diffusion-driven exchange between mobile and immobile can influence solute migration (Berkowitz et al. 2006). Several studies have shown that such Dual-Domain (DD) mass transfer processes can significantly influence breakthrough curves, solute storage, retardation and long-term release in heterogeneous subsurface systems (Lu et al. 2016; Foster et al. 2021; Li et al. 2022). Besides, soil matrix that hosts peaty horizons enriched with plant fragments (like the one under study) are particularly predisposed for DD approach due to the presence of immobile pore spaces and internal sorption processes that can further delay salt mobilization acting as long-term salt diffusion and other pollutants from these deposits (Ofori et al. 2025). Since the application of DD transport models is often constrained by the need for additional parameters describing mobile-immobile mass exchange, which may be difficult to quantify under limited data availability, ADE formulations are frequently adopted in practical groundwater modeling studies (Berkowitz et al. 2006). Despite their potential to provide a more realistic representation of solute transport in heterogeneous porous media, DD applications at field scale remain challenging because the parameters describing mobile-immobile mass exchange required additional measurements (Berkowitz et al. 2006; Lu et al. 2016; Foster et al. 2021; Li et al. 2022).

To fill this knowledge gap, in this study, different SEAWAT simulation scenarios were run to assess salinity dynamics in a reclaimed agricultural field of the Po River lowland, calibrated via a continuous field monitoring network. Specifically, the study aims (i) to build up two 2D density dependent models able to assess the role of DD, sorption and peat-related salt mass release in affecting spatial and temporal groundwater salinity distribution by testing multiple scenarios, and (ii) provide a useful tool for a quantitative assessment of the major processes driving agricultural fields salinization in complex heterogeneous environments.

2 Materials and Methods

2.1 Study Area and Monitoring Network

The study area falls within the Po River lowland (Italy), approximately 24 km from the Adriatic Sea (Fig. 1). This depressed, flat region is characterized by an intensive agricultural activity and is facing salinization problems as a legacy of the last marine transgression (Amorosi et al. 2008; Habakaramo Macumu et al. 2024). The coastal area presents a quite heterogeneous sediment origin, groundwater geochemistry and composition (Colombani et al. 2017) with freshwater swamps of fine organic sediments and brackish back barrier interbasins crossed by paleochannels (Bruno et al. 2022). Humid temperate climate characterizes the region with yearly average precipitation (2011–2040) of approximately 600 mm and a yearly average temperature (2011–2040) of 15 °C (Nistor and Mîndrescu 2019.). The shallow unconfined aquifer is hosted in heterogeneous alluvial sediments including silty-clay sediments, peat layers and sandy paleochannel bodies. Groundwater depth generally ranges between 1 and 0.5 m below ground level with very low hydraulic gradients and groundwater flows directed towards the drainage ditches and tile drains (Gaiolini et al. 2025b). The vadose zone is generally thin and composed of fine-grained organic-rich sediment. Moreover, the area underwent a series of hydrological and morphological changes during the Holocene paleoenvironmental evolution and the reclamation of inland deposits from the 15th to the 19th century (Bruno et al. 2022), leading to increased risk of flooding and groundwater salinization (Viero et al. 2019). For this study, two agricultural field plots were selected for hydrogeological investigations and monitoring. Specifically, in the field plot A1, groundwater and soil salinity are already reducing crop yields, whereas paleo-seawater trapped in the pore space of low permeability lenses together with salt release from halophytic fragments within the peaty horizons have rendered field plot A2 unsuitable for cultivation (Fig. 1).

To counteract salinization problems, avoid water-logging conditions and provide subirrigation, stainless steel tile drains of 5 cm diameter and with an interspacing of 10 m were installed in 2018 to drain away excess water and supply water to crops. Subirrigation was performed by opening the inlet valve from the main irrigation channel and placing removable weirs at the end of DR1 and DR2 ditches.

To investigate and track agricultural field conditions a monitoring network was set up including piezometers equipped with CTD Diver® datalogger measuring groundwater levels, temperature (T), electrical conductivity (EC) and converted salinity. CTD Diver® dataloggers were also placed in the main canals (DR1 and DR2) draining water from the field to track DR parameters (Fig. 1). Different piezometer installation depths below ground level

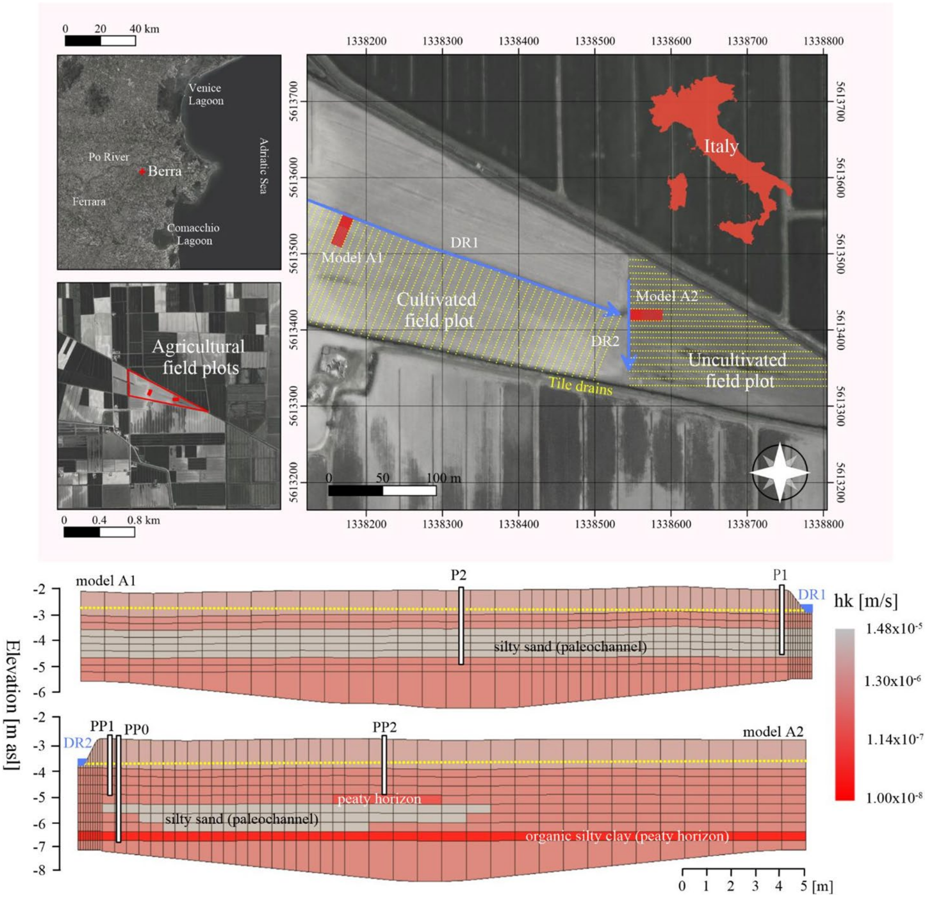

Fig. 1 Monitoring setup and model areas: (upper maps) plan view map of the two field plots and the tile drains (A1, cultivated maize and A2, uncultivated, saline, salt-tolerant weeds), showing tile drains, piezometers, ditches (DR1 and DR2); (lower profiles) discretization of 2D model domains and horizontal hydraulic conductivity distributions

among the monitoring network revealed the heterogeneity and complexity of the whole floodplain system. This comprehensive dataset was crucial to retrieve accurate data and build up physical based numerical models of groundwater flow and salt transport.

2.2 Model Setup and Boundary Conditions

The flow and transport simulations were performed by means of SEAWAT 4.2 (Langevin 2009) within the new graphical user interface PMWIN 11.0.6 (Chiang, 2025). SEAWAT 4.2 simulates variable-density groundwater flow and transport using the same finite-difference method to solve the groundwater flow equation (Guo and Langevin 2002):

$$\nabla \cdot \left[\rho \frac{\mu_0}{\mu} \mathbf{K}_0 \left(\nabla h_0 + \nabla z \frac{\rho - \rho_0}{\rho_0}\right)\right] = \rho S_{s,0} \frac{\partial h_0}{\partial t} + \theta \frac{\partial \rho}{\partial C} \frac{\partial C}{\partial t} - \rho_s q_s' \quad (1)$$

where ρ is the fluid density [ML^{-3}]; ρ_0 is the fluid density at the reference concentration and reference temperature [ML^{-3}]; μ is the dynamic viscosity [ML^{-1} T^{-1}]; μ_0 is the dynamic viscosity at the reference concentration and reference temperature [ML^{-1} T^{-1}]; K_0 is the hydraulic conductivity tensor of material saturated with the reference fluid [-]; h_0 is the hydraulic head measured in terms of the reference fluid of a specific concentration and temperature [L]; z is the upward coordinate direction aligned with gravity; t is time [T]; $S_{s,0}$ is the specific storage [L^{-1}]; θ is the porosity [-]; C is the salt concentration [ML^{-3}]; q'_s is a source or sink of fluid with density ρ_s [T^{-1}].

A DD transport approach (with sorption) was used to account for the extreme heterogeneity of the aquifer system, which is characterized by permeable sandy paleo-channels and low permeability peat and sandy-clay deposits. This approach considers the pore space partitioned into mobile and immobile domains and explicitly accounts for diffusive mass exchange between them, allowing simulation of delayed solute release from low-permeability horizons.

The exchange of the dissolved mass between the mobile and immobile domains is defined by the equation:

$$n_{im} \cdot \frac{\partial C_{im}}{\partial t} = \zeta \cdot (C_m - C_{im}) \tag{2}$$

where n_{im} [-] is the porosity of the immobile domain; C_{im} [ML^{-3}] is the solute concentration in the immobile domain; C_m [ML^{-3}] is the solute concentration in the mobile domain; and ζ [T^{-1}] is the first-order mass transfer rate between the mobile and immobile domains. Linear sorption was included to account for retardation of salt transport using the following equation:

$$C \bigcirc^{-} = C \cdot K_d \tag{3}$$

and assumes that the sorbed concentration $\overline{C}$ [ML^{-3}] is directly proportional to the dissolved concentration C [ML^{-3}]. The retardation factor R, is therefore independent of the concentration values and is calculated only once for each cell at the beginning of the simulation:

$$R = 1 + \frac{\rho_b \cdot K_d}{\theta} \tag{4}$$

where K_d [L^3M^{-1}] is the distribution coefficient and ρ_b [ML^{-3}] is the bulk density of the porous medium of the cell.

Two 2D vertical cross-sections were developed to represent dominant groundwater flow towards the drainage channels DR1 and DR2, neglecting lateral fluxes perpendicular to the sections. This approach (supported by the availability of monitoring data) was adopted to facilitate the simulation and focus on the vertical exchange processes between peaty horizons, paleochannels and drainage channels. The model domains extend 30 m each along the main flow lines and are discretized into 50 rows, and 10 layers with variable dimensions and thickness. The first layer was thicker than the others, to contain the water table variations and avoid dry cells that lead to convergence problem (Brunner et al. 2010). The grids were refined near drainage channels DR1 and DR2 to better capture their geomorphological features and surface-groundwater exchanges (Fig. 1b).

The top of the grids ranges from −2.9 to -1.9 m above sea level (asl), according to the Lidar 5 × 5 m DTM of the Emilia-Romagna Region. Horizontal hydraulic conductivity (HK) values found via rising head slug tests (Bouwer and Rice 1976) and infiltrometer tests, range between 1×10^{-8} m/s in silty clay-peaty horizons, to 1.48×10^{-5} m/s in paleochannel portions of the domains, consistent with values reported for fine alluvial sediments within the Po River floodplain (De Caro et al. 2017). Vertical hydraulic conductivity (VK) was set half of the horizontal component to account for internal layering. Effective porosity (n_e) and specific yield (S_y) were set between 0.05 (peaty horizons) and 0.2 (sandy paleochannel), while specific storage (S_s) was set 5×10^{-6} m^{-1} in the paleochannel and up to 1×10^{-3} m^{-1} in the peaty horizons (Bear and Braester 1972).

8-day average evapotranspiration rates were derived from the Moderate Resolution Imaging Spectroradiometer (MODIS) dataset (Running et al. 2019). The algorithm used is based on the logic of the Penman–Monteith equation, which includes inputs of daily meteorological reanalysis data and MODIS remotely sensed data products, such as vegetation property dynamics, albedo, and land cover (Mu et al. 2011). Data were downloaded from the MOD16A2GF model (Running et al. 2019) using the AppEEARS interface (AppEEARS, 2020). Recharge rates were estimated via Thornthwaite–Mather method (https://thornwaterbalance.com/) within WaterbalANce online app (Mammoliti et al. 2021) and subsequently manually adjusted according to continuous soil moisture content data nearby the water table (Gaiolini et al. 2025b); neglecting recharge when no soil moisture changes were recorded after a given rainfall event, or proportionally increasing the recharge rate with the soil moisture increase after a rainfall event. Temperature (Tm, degrees Celsius), and precipitation (P, millimeters) data used as inputs were derived from the on-site meteorological station. QGIS 3.36 software (http://www.qgis.org) was used to process the data by trimming the files, change coordinates and format to simulate them within the Recharge and Evapotranspiration Package (RCH and EVT), respectively.

Subirrigation during summer (June 12, 2024 - July 29, 2024) was simulated by injection wells (WEL package) in each cell representing a tile drain. Tile drains were modelled within the Drain Package (DRN), assuming an average depth of channels of -0.80 m below ground level. Surface drainage channels DR1 and DR2 were simulated within the Time-Variant Specified Head (CHB) using the corresponding 8-day averaged water levels monitoring data.

For transport, longitudinal dispersivity, vertical dispersivity and molecular diffusion were set 0.5 m, 0.05 m and 1×10^{-9} m^2/s, respectively. To recharge and evapotranspiration fluxes were assigned concentrations between 3.5 and 15 g/L according to the field plots halophyte vegetation cover found in literature (Ohrtman and Lair 2013), while the concentrations of the subirrigation flux were set consistently with measured values within the drainage channels (DR1 and DR2). Salinity was modelled as Total Dissolved Solids (TDS) reflecting the study objectives, which focus on comparing different modelling approach to simulate salinity dynamics, rather than represent geochemical action of different ionic species.

DD exchange coefficients including n_{im} (0.253), ζ (2×10^{-9}), distribution coefficient ($2.4 \times 10^{-4-4}.5 \times 10^{-4}$ m^3/kg) were set according to the values found by Ofori et al. (2025) in column experiments carried out in these sediments, while K_d values for dissolved salts in organic soils were derived from Li et al. 2022. Particular attention was given to the mass loading rate (MLR) within the peaty horizons, where different possible release rates were tested to account for different reactivity of the osmotic membranes constituting the variety of vegetation fragments present in the peaty horizons. In Model A2 higher values were applied to account for the higher salt release observed in the vegetation-rich peat deposits (Habakaramo Macumu et al. 2024; Ofori et al. 2025).

A sensitivity analysis was performed using single perturbation tests (±50% of the employed parameter values) on MLR, mass transfer rate, immobile porosity and distribution coefficient to ensure the resilience of the model's performance to changes in key transport parameters. To maintain model parsimony and avoid over-parametrization given the availability of data, spatial uniform DD and K_d parameters were adopted. The available data were insufficient to reliably constrain their spatial variability which would have introduced additional calibration uncertainty (Hill and Tiedeman 2007).

All the model parameters after the calibration procedure were reported in Table 1.

2.3 Numerical Simulations and Scenarios

Initially a quasi-steady state simulation was performed for one year under average recharge and evapotranspiration conditions to fully develop the salinity distribution throughout both the model domains. The final heads and concentrations were then imported as initial conditions for the subsequent transient run. The transient simulation covers the period from April 16, 2024 to May 5, 2025 discretized into 48 stress periods of 8-days each to capture variations in groundwater flow and salinity.

The flow models were calibrated via PEST (Doherty 2010) to match the observed groundwater levels recorded by the piezometers for the same period, optimizing hydraulic conductivity, recharge, drain conductance, subirrigation rate, specific storage and specific yield. Solute transport calibration was achieved manually adjusting transport coefficients and the MLR values to find the best compromised among multiple piezometers.

To assess the influence of DD exchange coefficient, sorption and MLR on salinity dynamics, several scenarios were tested. The three main simulations considered are: (i) DD trans-

Table 1 Models' flow and transport parameters after validation

Parameters	Values (range)	
	Model A1	Model A2
HK (m/s)	$1\times10^{-7a} - 1.48\times10^{-5a}$	$1\times10^{-8a} - 1.48\times10^{-5a}$
VK (m/s)	HK/2	HK/2
Ne (-)	$0.1^{b} - 0.20^{b}$	$0.05^{b} - 0.20^{b}$
Sy (-)	$0.1^{b} - 0.20^{b}$	$0.05^{b} - 0.20^{b}$
Ss (m^{-1})	$5\times10^{-6b} - 1\times10^{-3b}$	$5\times10^{-6b} - 1\times10^{-3b}$
Subirrigation rate (m^3/s)	5×10^{-7}	5×10^{-7}
Tile drain conductance (m^2/s)	2.5×10^{-8}	2.5×10^{-8}
Longitudinal dispersivity (m)	0.5	0.5
Vertical dispersivity (m)	0.05	0.05
Diffusion coefficient (m^2/s)	1×10^{-9}	1×10^{-9}
RCH concentration (g/L)	3.5	5
EVT concentration (g/L)	5	15
Mass loading rate	$2\times10^{-8} - 2\times10^{-7}$	$7.5\times10^{-8} - 3\times10^{-7}$
Distribution coefficient (m^3/kg)	4.5×10^{-4}	2.4×10^{-4}
Mass transfer coefficient	2×10^{-9a}	2×10^{-9a}

[a]Optimized values with PEST;[b]Values from Zheng et al. 2012

port with sorption, (ii) DD transport without sorption and (iii) ADE transport. Each of these simulations was run with and without additional MLR resulting in six model scenarios.

The models' performances were evaluated via classical statistical parameters (Moriasi et al. 2015), like: the determination coefficient (R^2), the Nash-Sutcliffe Efficiency (NSE), the Root Mean Square Error (RMSE) and the Percentage of Bias (PB).

Furthermore, Akaike Information Criteria (AIC) was used to penalize the inclusion of additional parameters and demonstrate that added complexity is justified (Poeter and Hill, 2007). The differences between the best model (AIC Δj) instead of the absolute values (AIC) were used to compare model scenarios (see Eqs. 1 and 2 in S1).

This approach allowed to infer how the inclusion of DD, sorption and salt release from peaty horizons affect the model performance metrics and the groundwater salinity patterns.

3 Results

3.1 Model Performances and Calculated Trends

Given the high degree of heterogeneity of sediments, both models were able to grasp the magnitude of groundwater levels over both the field plots (Fig. 2). In fact, good calibration performances were achieved with R^2 of 0.69, NSE of 0.62, RMSE values of 0.08 m

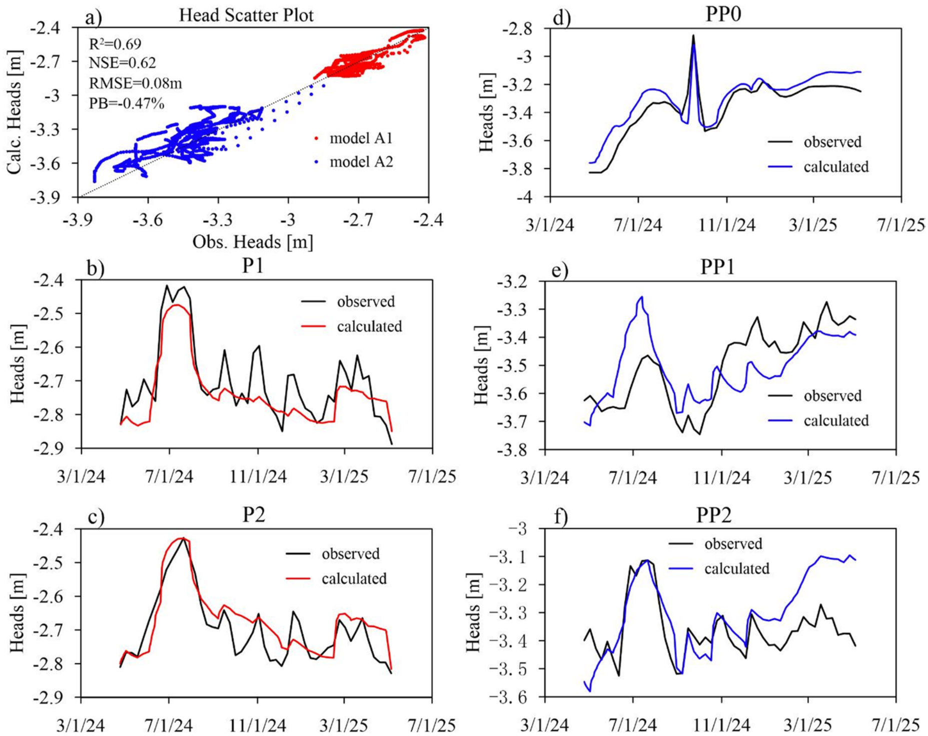

Fig. 2 Observed vs. simulated groundwater levels in the piezometers P1, P2, PP0, PP1 and PP2 together with the head scatter diagram and correlation coefficients

and a PB of 0.47% (Fig. 2a) providing a robust basis for subsequent transport simulations (Moriasi et al. 2015). Model A1 captured the water table rise induced by subirrigation (June 12, 2024 - July 29, 2024) and its later gradual decline (red lines in Fig. 2b-c). P1 and P2 quickly responded to rainfall input and direct connection to subsurface flow were not accurately simulated, but amplitudes and timing were well represented. On the other hand, in Model A2, the consistent presence of peaty horizons and vegetation fragments over the uncultivated field plot complicated groundwater responses. Despite this, general seasonal dynamics and hydrological processes (e.g., subirrigation, precipitation events) were well reproduced with varying accuracy across the piezometers (blue lines in Fig. 2d-e-f).

Figure 3 shows the calibration results of calculated versus measured salinity values, together with salinity trends in all the piezometers. Good performance metrics were computed (R^2 = 0.96, NSE = 0.95, RMSE = 0.28 g/L, PB = 0.35%, Fig. 3a) effectively assessing salinity dynamics throughout the system with relatively low error considering the presence of brackish to saline groundwater.

All the piezometers show quite stable salinity trends with variations from 0.2 to 1.5 g/L over the simulation. Like the calibration procedure for heads, the model accuracy diminished for the Model A2 (Fig. 3d-e-f) respect to Model A1 (Fig. 3b-c) due to the high heterogeneity of the subsurface media highlighted by different piezometers depths (PP0 > PP2>

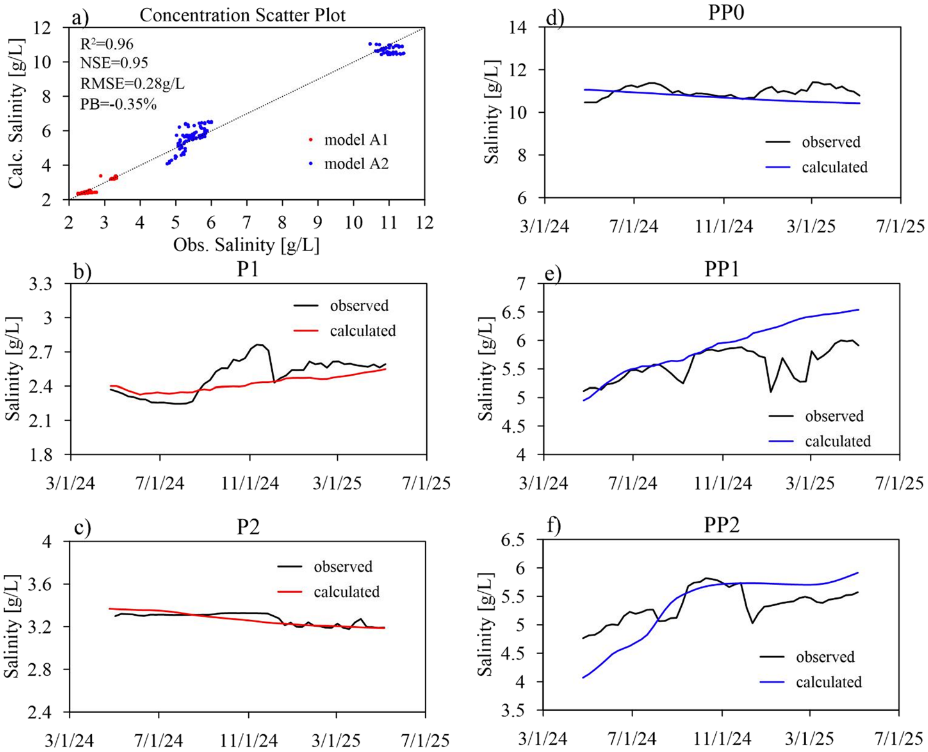

Fig. 3 Observed vs. simulated groundwater salinities in the piezometers P1, P2, PP0, PP1 and PP2 together with the concentration scatter diagram and correlation coefficients

PP1). Because of this, higher range of salinities values and fluctuations were not perfectly simulated with constant DD exchange parameters, but the calculated salinity generally mimicked the observed one capturing the overall magnitude and trend.

It must be underlined that the simplified 2D approach, together with the spatial uniform DD and sorption transport parameters, have limited the representation of short-term flow and salinity peaks neglecting lateral fluxes and concentration gradients among different layers of the subsurface system affecting the calibration results.

The sensitivity analysis shows that the models are robust to moderate perturbations of DD transport parameters (Table 2). However, model performances were clearly affected by changes in MLR, particularly in Model A2. A 50% reduction in MLR decreased NSE from 0.972 to 0.646 and increased RMSE from 0.436 to 1.553 g/L, highlighting the dominant role of peat-derived salt release in controlling groundwater salinity dynamics. The influence of the distribution coefficient (k_d) was intermediate implying the contribution of sorption processes to salinity buffering. In contrast, variations of the mass transfer coefficient and immobile porosity produced comparatively smaller changes in performance metrics, suggesting lower model sensitivity to these parameters.

3.2 Multiple Scenarios Testing

The challenges of simulating local vertical heterogeneities in field-scale models underscore the need for exploring different simulation approaches to understand salinity dynamics of peaty environments. To test this modeling approach, observed and simulated salinity trends were compared under the six different scenarios including: (i) DD transport with sorption, (ii) DD transport without sorption, (iii) ADE transport and the same three without considering additional MLR from peats (Fig. 4).

Across all piezometers within the two field plots the observed trends (dotted red lines) were best reproduced by the calibrated DD transport models with both sorption and MLR (solid red lines).

Not considering sorption leaded to higher salinity concentrations (purple lines) in shallower piezometers (P1, PP1, PP2 Fig. 4a-d-e) affected by higher rate of salt mobilization due to subirrigation and recharge events, whereas in deeper piezometers (P2, PP0 Fig. 4b-c) salinity trends are closer to observed values.

Table 2 Single parameter sensitivity analysis

	R^2		NSE		RMSE (g/L)		PB (%)	
	Model A1	Model A2	Model A1	Model A2	Model A1	Model A2	Model A1	Model A2
DD with sorption (validated)	0.939	0.975	0.927	0.972	0.111	0.436	-1.057	0.347
+50% mass loading rate	0.954	0.903	0.913	0.811	0.120	1.136	2.823	10.869
-50% mass loading rate	0.898	0.923	0.794	0.646	0.190	1.553	-4.354	-18.592
+50% mass transfer rate	0.922	0.960	0.879	0.932	0.143	0.683	-2.951	-4.575
-50% mass transfer rate	0.951	0.974	0.933	0.944	0.106	0.618	1.122	6.104
+50% immobile porosity	0.946	0.970	0.945	0.965	0.096	0.485	-0.600	0.427
-50% immobile porosity	0.923	0.977	0.884	0.977	0.140	0.395	-1.487	-0.447
+50% distribution coefficient	0.913	0.974	0.856	0.973	0.156	0.431	-1.901	-1.299
-50% distribution coefficient	0.942	0.961	0.937	0.950	0.102	0.582	-0.053	1.917

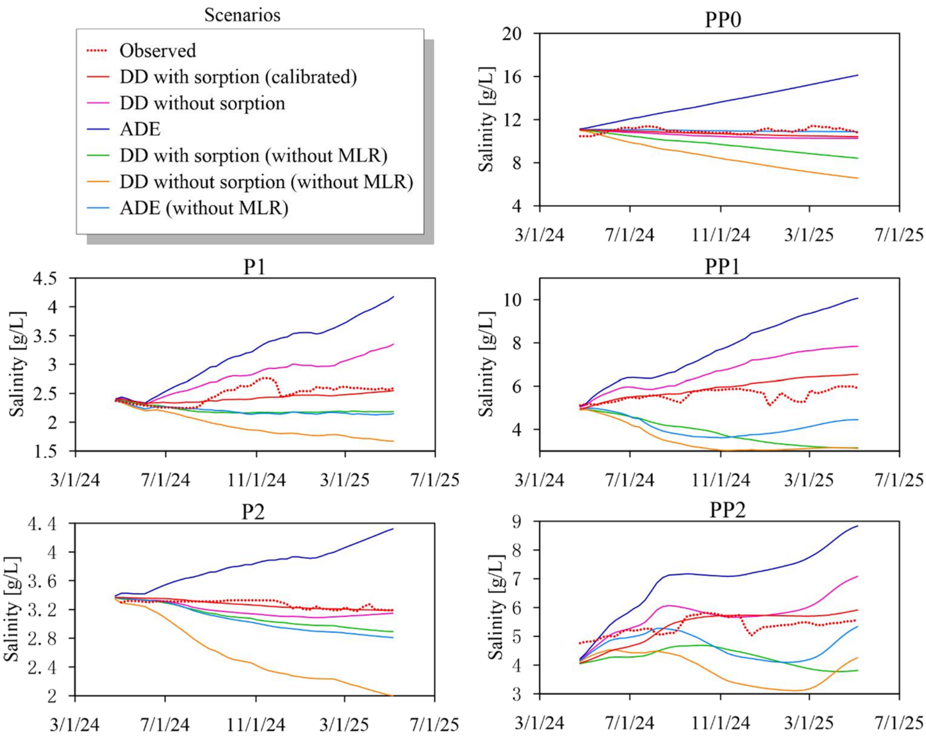

Fig. 4 Observed and simulated groundwater salinities in the piezometers P1, P2, PP0, PP1 and PP2 over multiple simulation scenarios

In contrast, ADE transport simulations (blue line) overestimated salinity accumulation over time across all piezometers predicting salinity values way higher than observed (e.g., above 16 g/L in PP0, Fig. 4c).

Scenarios without MLR simulate declining salinity trends over time not supported by observed data, underlining the role of including additional salt mass stocked within peaty horizons acting as a long-term source of salinity. It is worth noting that ADE scenario without MLR produced a concentration at piezometer PP0 that resemble the calibrated model. This is a clear example of how, in lack of sufficient observed data, an oversimplified approach seems to perform well while misrepresenting the underlying processes.

To gain a wider view of salinity dynamics of the lowland, salinity distribution maps at the end of each transport configurations were compared accounting for the same scenarios. The calibrated transport models resemble observed salinity data with concentrations in the range of 5–10 g/L across most of the profiles. Slightly higher values are within the deeper layers and peaty deposits, with lower values within paleochannel sandy horizons. Values up to 25 g/L were observed within the discharge zone of the domain at the groundwater-surface water interface. In contrast, DD transport without sorption and ADE approaches overestimate salinity in both model domains, displaying unrealistic salt accumulation and reflecting their inability to capture delayed release mechanisms particularly relevant in peaty horizons. MLR was confirmed as a key driver of salinity persistence across both the profiles and when deactivated salinity progressively declined. Particularly, the Model A2 (Fig. 5 right panels) enriched with peaty horizons and higher organic matter exhibits a stronger sensitivity to different approaches (Please refer to Supplementary Material).

Comparing model performance metrics quantified how the calibrated models better resembled observed data showing lower errors and bias, with higher correlation coefficients respect to other model approaches (see S1). Moreover, DD transport models including sorption and MLR show lower AIC values compared to other model scenarios demonstrating that improved performances are not related to the higher number of parameters compared with the ADE approach.

4 Discussion

The models allowed for an estimation of the salinity dynamics in both time and space, producing a comparison between trends (Fig. 4) and maps (Fig. 5) to quantify the key role of DD exchanges, sorption and peat-related salt mass on affecting salt mobilization and fluxes in these lowland environments. Salt mass budget calculations (Fig. 6a-b) confirmed that, in shallow coastal saline groundwater systems under subirrigation, the mobilization of salt stored within peaty horizons poses a high salinization risk for surface water resources (Gaiolini et al. 2025a; Habakaramo Macumu et al. 2024). High amounts of salt were released from both domains (544 and 1629 kg for the calibrated Model A1 and A2, respectively).

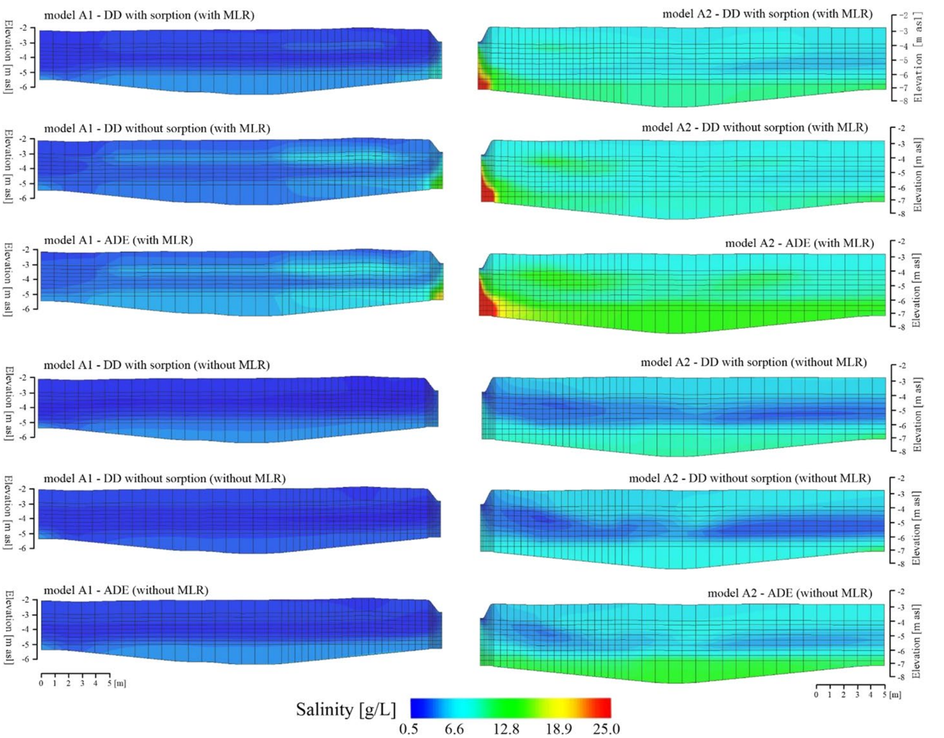

Fig. 5 Groundwater salinity distribution maps at the end of the simulations over multiple scenarios, elevation is in m asl

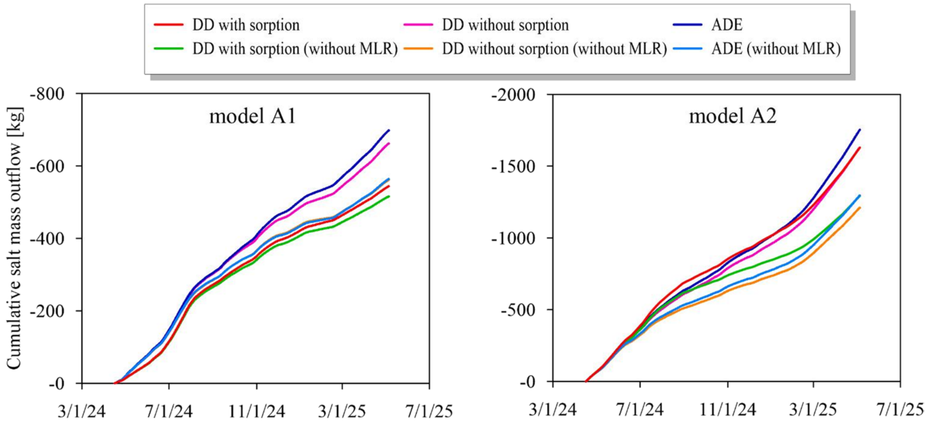

Fig. 6 Cumulative salt mass outflow over time from both the models A1 and A2 under the six tested scenarios

In both areas, ADE approaches estimate the highest cumulative salt mass outflow due to the lack of mobile-immobile domain diffusive transport preventing the models to reproduce the buffered salt release. In comparison, DD simulations show minor salt release highlighting the buffering and delaying role of immobile domain and sorption. This buffering capacity of the soil matrix was previously recognised (Ofori et al. 2025; Lu et al. 2016; Foster et al. 2021; Li et al. 2022), without any real application to salinization in peaty lowlands. It is interesting to notice that in field plot A2 (Fig. 6b) the calibrated model (red line) simulated a faster salt release than the no-sorption case scenario (purple line).

This can be explained by the stronger presence of peaty horizons in this field plot, where sorbed salts can be rapidly mobilized under changing concentration gradients due to recharge events and subirrigation, which was confirmed to be inefficient in freshening the system according to previous research (Su et al. 2005; Gaiolini et al. 2025b). Scenarios without MLR simulate consistently lower salt mass outflow underlining the significance of additional salt sources stored within peaty horizons enriched with vegetation fragments as previously postulated by Habakaramo Macumu et al. (2024).

These findings were crucial to understand how DD solute exchanges and sorption dynamics affect efficiency and timing of salt mobilization, not only improving the realism of the simulation, but also providing information on both groundwater and surface water quality. Most of the field-scale models did not account for the persistence of salts from peaty horizons by neglecting DD solutes exchanges and sorption mechanisms. This is due to the inherent difficulty to evaluate such parameters, which are rarely quantified in field conditions without a continuous monitoring network or elevated amount of spatially distributed data (Cao and Han 2024). However, incorporating these processes is particularly relevant in peaty cultivated environments prone to salinization like the Po River lowland, to improve irrigation management and support a sustainable agricultural production.

4.1 Assumptions and Limitations

Due to the availability of monitoring data and to facilitate the model comparative framework, several assumptions were adopted in the study. The 2D modelling approach, together with the spatial uniformity of the DD and sorption parameters, limits the models to reproduce short-term flow and salinity fluctuations related to lateral fluxes and concentration gradients among different layers. Nonetheless, the distribution of the tile drains perpendicular to the drainage ditches in both fields exert a strong influence on the groundwater flow field making the assumption of 2D flow and transport along the selected transects plausible. This assumption was supported by complex 3D models performed in similar agricultural field that confirmed the strong influence of tile drains on the groundwater flow field (De Schepper et al. 2015; Rozemeijer et al. 2010). In addition, linear isotherm sorption was considered within the simulations, while soil matrix often present non-linear sorption behaviours (Wen et al. 2012) which should be explored in future studies. Therefore, even if the models were constrained by field and laboratory measured data, the 2D mass balance calculation should be interpreted with caution when considering water managing strategies.

Future research should account for this subsurface spatial heterogeneity and geochemical complexity (Habakaramo Macumu et al. 2024) and explore 3D specific transport simulations using multicomponent reactive transport models, to better delineate the influence of pyrite oxidation and other relevant biogeochemical processes active at the site (Ofori et al. 2025). Moreover, the sensitivity analysis indicate that the model performances were considerably more sensitive to changes in MLR, particularly in the peat-rich Model A2. Therefore, future investigations should also prioritize improved characterization of salt storage and release mechanism within peat deposits to reduce uncertainties.

Since the same assumptions were applied to all the tested scenarios, this modelling approach identified the best formulation to reproduce groundwater dynamics and salinity persistence under identical conditions (as supported by statistical analysis and information criteria). This approach improved the representation of salt transport processes, better capturing key phenomena driving salinization and adding management relevance.

5 Conclusions

This study demonstrated the importance of including DD solutes transport, sorption processes, and additional salt mass stocked in peaty horizons to improve simulations realism and agricultural management relevance. The continuous field monitoring allowed for a proper setting and calibration of two density-dependent solute transport models that captured groundwater flow and salinization processes, despite the assumption of 2D groundwater flow and solute transport along the tile drain transects. The DD models better reproduced observed groundwater heads and salinity variations in comparison to ADE simulations, which overestimated salinity accumulation. The same happened without considering sorption, which introduced an additional buffering mechanism to capture the salt release rate during subirrigation. In contrast, simulations without additional salt mass simulated a declining salinity, not supported by the observed data. The MLR was found a key parameter accounting for salinity persistence and underlining the role of salt mass stocked within peaty horizons acting as a long-term source of salinity. The salt mass budget calculations confirmed that subirrigation was inefficient in freshening peaty groundwater systems. The scenario modelling found important salt export differences among the simulated approaches; underlining the importance of including DD, sorption and MLR to quantify salinization patterns in these environments and their expected freshening timeframe to guide proper decision-making towards a sustainable water resources management.

Supplementary Information The online version contains supplementary material available at https://doi.org/10.1007/s40710-026-00851-0.

Author Contributions All authors contributed to the study conception and design. Material preparation, data collection and analysis were performed by M.G. and N.C. The first draft of the manuscript was written by M.G. and all authors commented on previous versions of the manuscript. All authors read and approved the final manuscript.

Funding Open access funding provided by Università Politecnica delle Marche within the CRUI-CARE Agreement. We acknowledge financial support under the National Recovery and Resilience Plan (NRRP), Mission 4, Component 2, Investment 1.1, Call for tender No. 104 published on 2.2.2022 by the Italian Ministry of University and Research (MUR), funded by the European Union – NextGenerationEU, Project Title NO3EXCESS - Nitrogen Origin, EXport and Cycling in coastal irrigatEd SettingS – CUP F53D23002160001 - Grant Assignment Decree No. 2022AKA3HL adopted on 30/06/2024 by the Italian Ministry of University and Research (MUR).

Data Availability No datasets were generated or analysed during the current study.

Declarations

Competing Interests The authors declare no competing interests.

References

Amorosi A, Fontana A, Antonioli F, Primon S, Bondesan A (2008) Post-LGM sedimentation and holocene shoreline evolution in the NW adriatic coastal area. GeoActa 7:41–67. https://hdl.handle.net/11577/2470766

AppEEARS Team (2020) Application for extracting and exploring analysis ready samples (AppEEARS); Ver. 2.54.1. NASA EOSDIS land processes distributed active archive center (LP DAAC); USGS/earth resources observation and science (EROS) center: Sioux Falls, SD, USA. https://lpdaacsvc.cr.usgs.gov/appeears (accessed in June 2025)

Bear J, Braester C (1972) On the flow of two immscible fluids in fractured porous media. Dev Soil Sci 2:177–202. https://doi.org/10.1016/S0166-2481(08)70538-5

Berkowitz B, Cortis A, Dentz M, Scher H (2006) Modeling non-Fickian transport in geological formations as a continuous time random walk. Rev Geophys 44(2). https://doi.org/10.1029/2005RG000178

Bonaldo D, Bellafiore D, Ferrarin C, Ferretti R, Ricchi A, Sangelantoni L, Vitelletti ML (2023) The summer 2022 drought: a taste of future climate for the Po valley (Italy)? Reg. Environ Change 23(1):1. https://doi.org/10.1007/s10113-022-02004-z

Bouwer H, Rice RC (1976) A slug test for determining hydraulic conductivity of unconfined aquifers with completely or partially penetrating wells. Water Resour Res 12(3):423–428. https://doi.org/10.1029/WR012i003p00423

Brunner P, Simmons CT, Cook PG, Therrien R (2010) Modeling surface water-groundwater interaction with MODFLOW: Some considerations. Groundwater 48(2):174–180. https://doi.org/10.1111/j.1745-6584.2009.00644.x

Bruno L, Campo B, Hajdas I, Hong W, Amorosi A (2022) Timing and mechanisms of sediment accumulation and pedogenesis: Insights from the Po Plain (northern Italy). Palaeogeogr Palaeoclimatol Palaeoecol 591:110881. https://doi.org/10.1016/j.palaeo.2022.110881

Cao G, Han D (2024) Reversibility of seawater intrusion in a coastal aquifer: Insights from long-term field observation and numerical modeling. J Hydrol 638:131470. https://doi.org/10.1016/j.jhydrol.2024.131470

Chiang E, MODPATH (2025) User Guide for Processing Modflow Version 11.0.6 — A graphical user interface for MODFLOW, GSFLOW, MT3D, PEST, PESTPP-IES, SEAWAT, and ZoneBudget. Simcore Software. https://www.simcore.com/files/pm/v11/pm11.0.5pdf

Colombani N, Cuoco E, Mastrocicco M (2017) Origin and pattern of salinization in the Holocene aquifer of the southern Po Delta (NE Italy). J Geochem Explor 175:130–137. https://doi.org/10.1016/j.gexplo.2017.01.011

Dang X, Gao M, Wen Z, Jakada H, Hou G, Liu S (2020) Evolutionary process of saline groundwater influenced by palaeo-seawater trapped in coastal deltas: A case study in Luanhe River Delta, China. Estuar Coastal Shelf Sci 244:106894. https://doi.org/10.1016/j.ecss.2020.106894

De Caro M, Crosta GB, Frattini P, Perico R, Volpi G (2017) Hydrofacies reconstruction of glaciofluvial aquifers and groundwater flow modelling in a densely urbanized area under changing climatic conditions. Hydrol Earth Syst Sci Discuss 1–44. https://doi.org/10.5194/hess-2017-555

De Schepper G, Therrien R, Refsgaard JC, Hansen AL (2015) Simulating coupled surface and subsurface water flow in a tile-drained agricultural catchment. J Hydrol 521:374–388. https://doi.org/10.1016/j.jhydrol.2014.12.035

Diersch HJG (2005) FEFLOW software - finite element subsurface flow and transport simulation system - reference manual. WASY GmbH, p 292

Doherty J (2010) PEST-model-independent parameter estimation. Version 12. Watermark computing. Australia. http://www.pesthomepage.org/ (accessed in June 2025)

Erostate M, Huneau F, Garel E, Ghiotti S, Vystavna Y, Garrido M, Pasqualini V (2020) Groundwater dependent ecosystems in coastal Mediterranean regions: Characterization, challenges and management for their protection. Water Res 172:115461. https://doi.org/10.1016/j.watres.2019.115461

Foster A, Trautz AC, Bolster D, Illangasekare T, Singha K (2021) Effects of large-scale heterogeneity and temporally varying hydrologic processes on estimating immobile pore space: a mesoscale-laboratory experimental and numerical modeling investigation. J Contam Hydrol 241:103811. https://doi.org/10.1016/j.jconhyd.2021.103811

Gaiolini M, Colombani N, Chierici V, Montanari L, Mastrocicco M (2025a) Numerical modelling of groundwater level and salinity evolution in a low-lying coastal area under intensive agricultural activity. Water Resour Manage 39(4):1747–1761. https://doi.org/10.1007/s11269-024-04044-y

Gaiolini M, Sbarbati C, Ofori A, Habakaramo Macumu P, Gervasio MP, Tamisari E, Vincenzi F, Soana E, Castaldelli G, Piscopo V, Mastrocicco M, Colombani N (2025b) Salt migration and export via subsurface irrigation in a saline reclaimed landscape of the Po River lowland (Italy). J. Hydrol., in press. https://doi.org/10.1016/j.jhydrol.2025.134563

Gervasio MP, Soana E, Granata T, Colombo D, Castaldelli G (2022) An unexpected negative feedback between climate change and eutrophication: higher temperatures increase denitrification and buffer nitrogen loads in the Po River (Northern Italy). Environ Res Lett 17(8):084031. https://doi.org/10.1088/1748-9326/ac8497

Guo W, Langevin CD (2002) User's guide to SEAWAT: a computer program for simulation of three-dimensional variable-density ground-water flow (Vol. 1, No. 434). US Geological Survey

Habakaramo Macumu P, Gaiolini M, Ofori A, Mastrocicco M, Colombani N (2024) Additional sources of salinity and heavy metals from plant residues of peaty horizons in the Po River lowland (Italy). Sci Total Environ 957:177671. https://doi.org/10.1016/j.scitotenv.2024.177671

Hill MC, Tiedeman CR (2007) Effective groundwater model calibration: with analysis of data, sensitivities, predictions, and uncertainty. Wiley

Hussain MI, Farooq M, Muscolo A, Rehman A (2020) Crop diversification and saline water irrigation as potential strategies to save freshwater resources and reclamation of marginal soils—A review. Environ Sci Pollut Res 27(23):28695–28729. https://doi.org/10.1007/s11356-020-09111-6

Khondoker M, Mandal S, Gurav R, Hwang S (2023) Freshwater shortage, salinity increase, and global food production: A need for sustainable irrigation water desalination—A scoping review. Earth 4(2):223–240. https://doi.org/10.3390/earth4020012

Langevin CD (2009) SEAWAT: a computer program for simulation of variable-density groundwater flow and multi-species solute and heat transport. U S Geol Surv Fact Sheet FS 2009–3047 2. https://doi.org/10.3133/fs20093047

Li H, Werner AD, Lu C (2022) Coupled effects of density and dual-domain mass transfer on aquifer storage and recovery. Water Resour Res 58(8):e2021WR031445. https://doi.org/10.1029/2021WR031445

Lu C, Shi L, Chen Y, Xie Y, Simmons CT (2016) Impact of kinetic mass transfer on free convection in a porous medium. Water Resour Res 52(5):3637–3653. https://doi.org/10.1002/2016WR018724

Majeed A, Muhammad Z (2019) Salinity: a major agricultural problem—causes, impacts on crop productivity and management strategies. Plant abiotic stress tolerance: Agronomic Mol Biotechnol approaches 83–99. https://doi.org/10.1007/978-3-030-06118-0_3
Mammoliti E, Fronzi D, Mancini A, Valigi D, Tazioli A (2021) WaterbalANce, a WebApp for thornthwaite–mather water balance computation: comparison of applications in two European watersheds. Hydrology 8(1):34. https://doi.org/10.3390/hydrology8010034
Meyer R, Engesgaard P, Sonnenborg TO (2019) Origin and dynamics of saltwater intrusion in a regional aquifer: Combining 3-D saltwater modeling with geophysical and geochemical data. Water Resour Res 55(3):1792–1813. https://doi.org/10.1029/2018WR023624
Moriasi DN, Gitau MW, Pai N, Daggupati P (2015) Hydrologic and water quality models: Performance measures and evaluation criteria. Trans ASABE 58(6):1763–1785. https://doi.org/10.13031/trans.58.10715
Mu Q, Zhao M, Running SW (2011) Improvements to a MODIS global terrestrial evapotranspiration algorithm. Remote Sens Environ 115(8):1781–1800. https://doi.org/10.1016/j.rse.2011.02.019
Nistor MM, Mîndrescu M (2019) Climate change effect on groundwater resources in Emilia-Romagna region: An improved assessment through NISTOR-CEGW method. Quatern Int 504:214–228. https://doi.org/10.1016/j.quaint.2017.11.018
Ofori A, Alessandrino L, Vipin R, Mastrocicco M, Colombani N (2025) Flow-interruption experiments to quantify trace elements leaching from a shallow saline aquitard. Sci Tot Environ 1004:180823. https://doi.org/10.1016/j.scitotenv.2025.180823
Ohrtman MK, Lair KD (2013) Tamarix and salinity: an overview. Tamarix: a case study of ecological change in the American West. Oxford University Press, New York, pp 123–145
Poeter EP, Hill MC (2007) MMA, a computer code for multi-model analysis (No. 6-E3). Geological Survey (US). https://doi.org/10.3133/tm6E3
Rozemeijer JC, Van Der Velde Y, McLaren RG, Van Geer FC, Broers HP, Bierkens MFP (2010) Integrated modeling of groundwater–surface water interactions in a tile-drained agricultural field: The importance of directly measured flow route contributions. Water Resour Res 46:W11537. https://doi.org/10.1029/2010WR009155
Running S, Mu Q, Zhao M, Moreno A (2019) MOD16A2GF MODIS/terra net evapotranspiration gap-filled 8-day L4 global 500 m SIN Grid V006. NASA EOSDIS Land Processes DAAC. 20. https://doi.org/10.5067/MODIS/MOD16A2GF.006. (accessed in June 2025)
Sanga DL, Mwamahonje AS, Mahinda AJ, Kipanga EA (2024) Soil salinization under irrigated farming: A threat to sustainable food security and environment in semi-arid tropics. J Agric Sci Pract 9(3):32–47. https://doi.org/10.31248/JASP2024.468
Seibert SL, Greskowiak J, Bungenstock F, Freund H, Karle M, Meyer R, Oude Essink GHP, van Engelen J, Massmann G (2023) Paleo-hydrogeological modeling to understand present-day groundwater salinities in a low-lying coastal groundwater system (northwestern Germany). Water Resour Res 59(4):e2022WR033151. https://doi.org/10.1029/2022WR033151
Su N, Bethune M, Mann L, Heuperman A (2005) Simulating water and salt movement in tile-drained fields irrigated with saline water under a Serial Biological Concentration management scenario. Agric Water Manage 78(3):165–180. https://doi.org/10.1016/j.agwat.2005.02.003
Viero DP, Roder G, Matticchio B, Defina A, Tarolli P (2019) Floods, landscape modifications and population dynamics in anthropogenic coastal lowlands: The Polesine (northern Italy) case study. Sci Tot Environ 651:1435–1450. https://doi.org/10.1016/j.scitotenv.2018.09.121
Voss CI (1984) SUTRA: a finite-element simulation model for saturated unsaturated, fluid-density-dependent ground-water flow with energy transport or chemically reactive single-species solute transport. US Geol. Surv. Water-Resources Invest Rep 84(4369). https://doi.org/10.3133/wri844369
Wen Y, Su LM, Qin WC, Fu L, He J, Zhao YH (2012) Linear and non-linear relationships between soil sorption and hydrophobicity: Model, validation and influencing factors. Chemosphere 86(6):634–640. https://doi.org/10.1016/j.chemosphere.2011.11.001
Yang H, Yang T, Yang F, Yang X (2023) Assessment of groundwater salinization impact in coastal aquifers based on the shared socioeconomic pathways: An integrated modeling approach. Environ Res 234:116618. https://doi.org/10.1016/j.envres.2023.116618
Zörb C, Geilfus CM, Dietz KJ (2019) Salinity and crop yield. Plant Biol 21:31–38. https://doi.org/10.1111/plb.12884